

I.M. Pazukha, D.O. Shuliarenko, O.V. Pylypenko, M.S. Ovrutskyi, L.V. Odnodvoretz
**Concentration and Size Effects in Electrophysical Properties of Thin
Films Based on Permalloy and Silver**

Sumy State University, Sumy, Ukraine, iryua.pazukha@gmail.com

Complex study of electrophysical properties (the electrical resistivity ρ and the temperature coefficient of resistance (TCR) β) of thin-film samples based on ferromagnetic alloy $\text{Ni}_{80}\text{Fe}_{20}$ (permalloy) and noble metal Ag in a wide composition range and within the range of thickness 20 - 100 nm is done. Thin films were obtained by the method of electron-beam co-evaporation technique at room temperature. Their composition was investigated using the method of X-ray spectrometry. The phase state was analyzed by the electron diffraction method. It was demonstrated that the crystal structure of thin films stays unchanged during the annealing process to 500 K. The size and concentration dependences of ρ and β values were obtained. The corresponding maximum and minimum at the concentration of Ag atoms of 50 - 60 at.% observed at the dependences $\rho(c_{\text{Ag}})$ and $\beta(c_{\text{Ag}})$. Size dependences $\rho(d)$ and $\beta(d)$ associated with the size effects in thin-film materials.

Keywords: thin-film, electrical resistivity, temperature coefficient of resistance, size effect, concentration effect.

Received 27 April 2020; Accepted 15 June 2020.

Introduction

Magnetoresistive properties of the ferromagnetic/nonmagnetic thin-film systems are studied intensively by many researchers [1-4]. In these systems, the direction of conducting electrons movements depends on the direction of the applied magnetic field. As a result, many magnetoresistive effects observed in these systems, such as giant magnetoresistance (GMR) [5] and Hall effect [6]. The previous study revealed that the magnitude of the GMR effect depends on technological parameters (vacuum conditions, condensation speed, substrate temperature, etc.), and type of the magnetic systems (multilayer, spin-valve or granular alloy). These allow expands a range of ferromagnetic/nonmagnetic systems applications for electronic systems [7, 8].

Recently, we have reported on the effect of the addition of non-magnetic Ag atoms on magnetoresistive properties of $\text{Ni}_{80}\text{Fe}_{20}$ ferromagnetic thin-film alloy. The effect was found to depend on thin film composition and takes the maximum value of about 1.45 % at room temperature and $c_{\text{Ag}} = 60$ at.% in the as-deposited state [9]. At the same time, it should attend that the resistivity

is one of the fundamental parameters that affect the transport, strain, magnetoresistive, etc. properties of the ferromagnetic/nonmagnetic thin-film systems. So, the purpose of this paper is the investigation of the concentration and size effects in electrophysical properties of thin films based on ferromagnetic alloy $\text{Ni}_{80}\text{Fe}_{20}$ (permalloy) and Ag.

I. Experimental procedure

Thin-film samples were prepared by the method of electron-beam co-evaporation of permalloy (Py) and Ag at room temperature in the vacuum chamber (a base pressure 10^{-4} Pa). The samples were deposited on a series of amorphous glass-ceramic substrates, which were placed in a vacuum chamber in a row. In such a location, each substrate placed at a different distance from Py and Ag sources (Fig. 1). The condensation rate was 0.1 nm/s for Py and Ag. As a result, the series of samples with a concentration of Ag atoms in the range of 20 - 85 at.% were obtained in one deposition run. The total thickness of the thin films changed within the range

from 20 to 100 nm. The thickness was monitored by two in situ quartz resonators. The calculation of the total thickness of the films was made based on the equations [11]:

$$d_1 = d_{01} \cdot \left[1 + \left(\frac{l_1}{h} \right)^2 \right]^{-\frac{3}{2}}, \quad d_2 = d_{02} \cdot \left[1 + \left(\frac{l_2}{h} \right)^2 \right]^{-\frac{3}{2}},$$

where d_0 is the thickness of the thin-film in the point under the evaporator, h is a high of evaporator under the quartz resonator, l_1 and l_2 are the distance from the point, in which the thickness determinates, to first and second quartz resonators respectively.

Composition and elemental analysis of thin films was done using Scanning electron microscope equipment with an energy dispersive detector to perform the X-ray spectrometry Tescan VEGA3.

The annealing performed in a vacuum chamber at 10^{-4} Pa. For an investigation of electrophysical properties, the samples after deposition annealed during the two-cycle “heating ↔ cooling” within the temperature range 300 - 550 K. For annealing, the automotive regime realized. It allows controlling the heating rate of the samples, record, and process the experimental data. The value of temperature coefficient of resistance (TCR) has been calculated on the base of temperature dependences of resistivity by the equation:

$\beta = (1/\rho_{in}) \cdot (\Delta\rho/\Delta T)$, where ρ_{in} is the initial value of resistivity, $\Delta T = 5$ K.

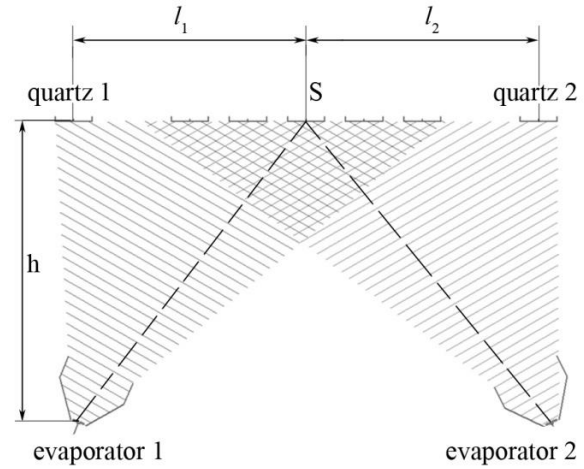


Fig. 1. The geometry of the system: evaporators (1, 2), substrates, quartz resonators, for preparation thin-film systems based on Py and Ag in wide concentration range, and the scheme for concentration calculation.

To examine crystal structure and phase state of thin films before and after annealing, the samples were evaporated into microscopic copper grids with a

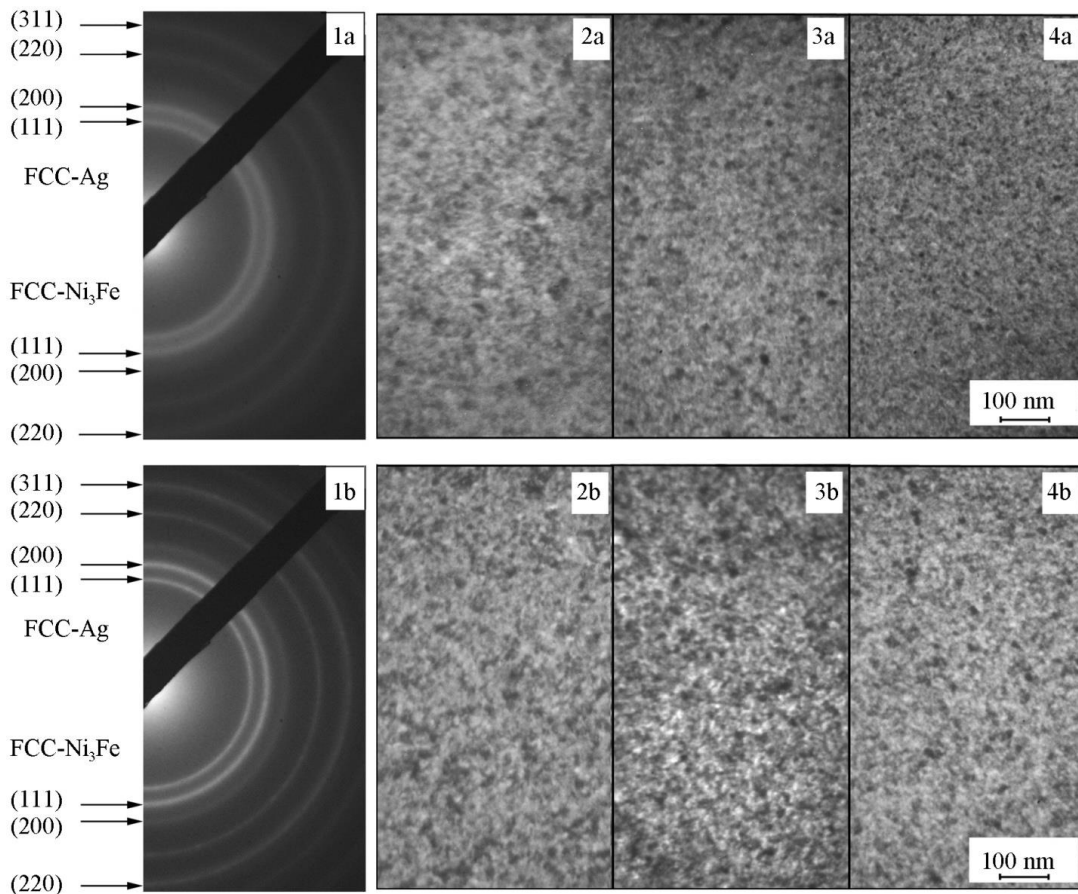


Fig. 2. Diffractions (1a, 1b) and bright field TEM images (2a-4a, 2b-4b) for thin-film systems based on Py and Ag with the total thickness of 50 nm before (a) and after annealing to 500 K (b) at the $c_{Ag} = 60$ (1, 2), 40 (3), and 20 at.% (4).

previously deposited carbon layer. The analysis was done by the TEM-125K microscope in the bright-field and diffraction modes using the method of transmission electron microscopy.

II. Results and discussion

To analyze the concentration and size effects in the electrophysical properties of thin films based on Py and Ag, it is important to know of their crystal structure in as-deposited and annealed states. Besides, the morphology of thin films is different in samples with various compositions and may cause change to the resistivity value. So it is necessary to study the crystal structure of investigated thin films too.

Fig. 2 shows the typical diffraction image and evaluation of phase state at the concentration change during annealing to 500 K for thin-film systems based on Py and Ag with a total thickness of 50 nm. According to our analysis, as-deposited films have a two-phase state, which corresponds to the face-centered cubic (FCC) Ni₃Fe and FCC-Ag structure with a lattice constant 0.355 nm and 0.408 nm, respectively. After annealing to

500 K, the phase state remains unchangeable. It observed a slight increase in the lattice parameter to 0.357 nm for FCC-Ni₃Fe and 0.408 nm for FCC-Ag.

Positions (2)-(4) in Fig. 2 demonstrate the variation of the phase state at the decrease of the concentration of Ag atoms. The decrease of c_{Ag} from 60 to 20 at.% leads to the reduction of the crystallite mean size, while their size slightly changes at the annealing to 500 K.

The resistivity and temperature coefficient of resistance as a function of the temperature for thin-film systems based on Py and Ag with various concentrations of atoms of noble metal are presented in Fig. 3. The value of resistivity for as-deposited samples with $d = 50$ nm and $c_{Ag} = 25$ and 80 at.% ranging from $6.8 \cdot 10^{-7}$ to $3.0 \cdot 10^{-7}$ Ohm·m. This is intermediate value between corresponding values for Py ($\rho = 8 \cdot 10^{-7}$ Ohm·m) [10] and pure Ag ($\rho = 0.4 \cdot 10^{-7}$ Ohm·m) [11] with $d = 60$ nm. This difference can be explained by the different crystal structures of permalloy and pure Ag thin films. The crystal structure of pure Ag thin films in the as-deposited state consists of the crystallites with the mean size of 20 nm [11], or even 50 nm [12], depending on the preparation method. At the same time, the crystal structure of Py thin films in the as-deposited state is

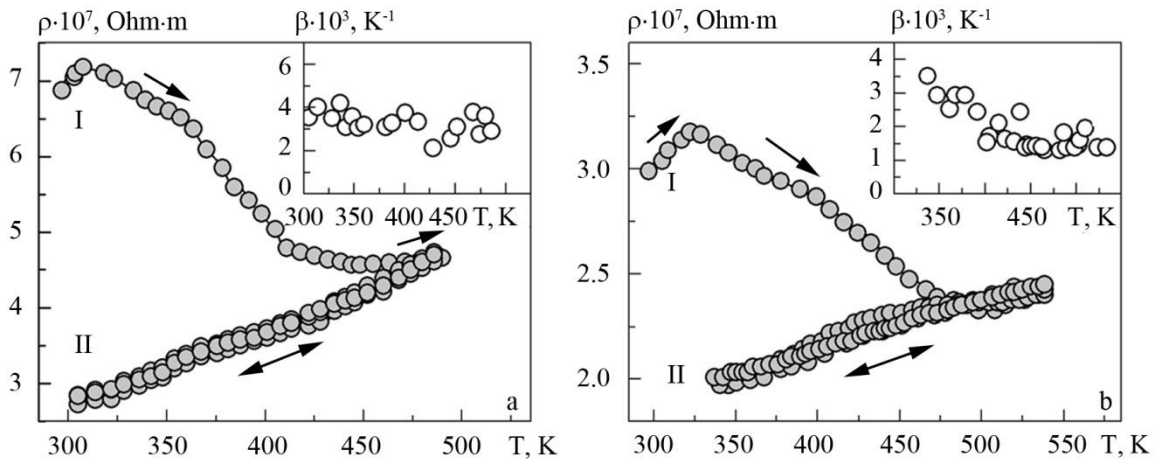


Fig. 3. Electrical resistivity and TCR (in the insert) as a function of the annealing temperature for the thin-film structures based on Py and Ag at the $c_{Ag} = 25$ (a) and 80 at.% (b) with a total thickness of 50 nm.

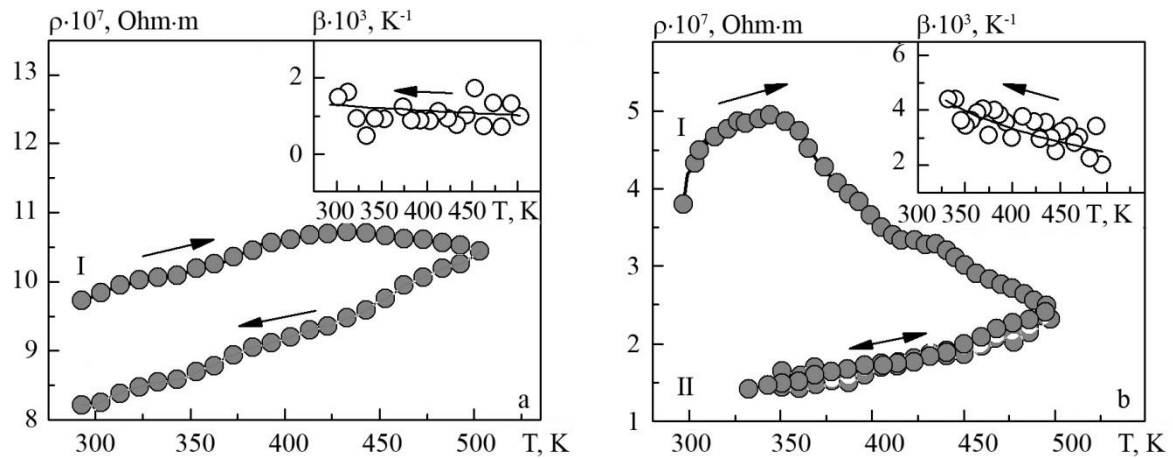


Fig. 4. Resistivity and TCR (in the insert) as a function of the annealing temperature for the thin-film structures based on Py and Ag with $c_{Ag} = 60$ at.% (b) at a total thickness of $d = 20$ (a) and 80 nm (b).

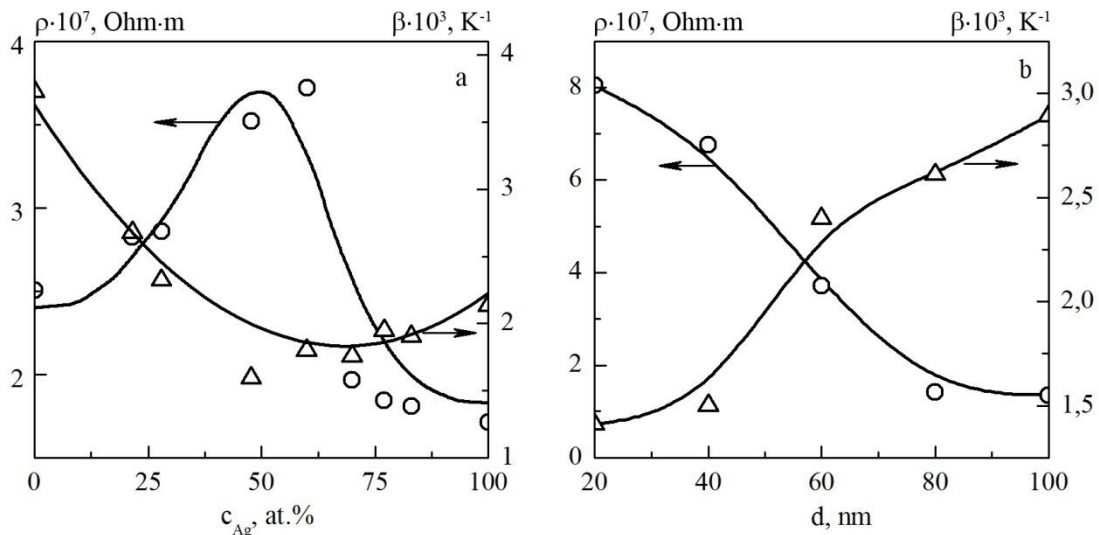


Fig. 5. The electrical resistivity and TCR as a function of the concentration of the Ag atoms (a) and the total thickness of the thin films (b).

typical for ferromagnetic materials labyrinth structure with the mean crystallite size that not exceeding 6 nm [10, 13]. It is clear that the resistivity for as-deposited films based on Py and Ag tends to the value of ρ for permalloy thin films. In our opinion, the main reason for this is a significant reduction of the crystallites that belong to the FCC-Ag phase during the condensation process.

An irreversible decrease in resistance observed during the annealing process. There is a result of the structural defects healing and an increase in the crystallite sizes. The following process of the cooling of the samples causes the appearance of $\rho(T)$ dependence, which typical for metals materials. The value of ρ is linear decreases at the cooling to the room temperature. At the graph TCR vs. annealing temperature, the dependence $\beta \sim 1/T$ is observed (see inserts in Fig. 3). At this, the increase of c_{Ag} concentration from 25 to 80 at.% does not change the general nature of $\rho(T)$ and $\beta(T)$ dependences.

At the same time, the decrease in the total thickness of the samples to 20 nm influences on the external view of the $\rho(T)$ dependence at the first cycles of cooling. The protracted nature of the temperature dependence of electrical resistivity, in this case, gives evidence of the defective structure of the thin films (a relatively large concentration of vacancies and stacking faults) and very small crystallite sizes.

Resulting evaluation of ρ and β at the increase of c_{Ag} and the total thickness for investigated thin films presented in Fig. 5. It is clear that the concentration dependences of resistivity and TCR (Fig. 5a) characterized by the presence of corresponding maximum and minimum within the $c_{Ag} = 50 - 60$ at.%. At lower and higher concentration, the reduction of ρ value is observed. That is associated with the change of the crystallites size at the concentration of noble metal grows. For the thin-film with low c_{Ag} , the Ag grain growth stagnation occurs as a result of their isolation in the ferromagnetic matrix. In the case of high concentration of Ag atoms, the crystal structure of the

thin films can be described as small ferromagnetic particles, which randomly distributed in the volume of non-magnetic material.

The value of electrical resistivity and TCR for thin films based on Py and Ag at $c_{Ag} = \text{const}$ also depends on the total thickness of the samples (Fig. 5b). The growth of the thickness from 20 to 100 nm leads to a decrease in the resistivity value in 5 - 6 times, while the TCR value increases in 2 - 3 times. In the case when the concentration of non-magnetic atoms is constant, such a change of ρ and β is associated with the size effects in thin-film materials [14].

Conclusion

The concentration and size effects in electrophysical properties of thin films based on ferromagnetic alloy Ni₈₀Fe₂₀ and non-magnetic metal Ag have been studied. The values of resistivity and TCR was found to depend on thin-film composition and takes the corresponding maximum and minimum at the $c_{Ag} = 50 - 60$ at.%. That is associated with the change of structural defect concentration and mean crystallite size. Their variation with the total thickness change in the range from 20 to 100 nm has been discussed for the concentration of Ag atoms of 60 at.%. At the growth of the total thickness of the samples, the size effect appears. As a result, the value of ρ decreases from $8 \cdot 10^{-7}$ to $1.35 \cdot 10^{-7}$ Ohm-m within the thickness range of 20-100 nm, while the value of β increases from $1.40 \cdot 10^{-3}$ to $2.90 \cdot 10^{-3}$ K⁻¹.

This work was funded by the State Program of the Ministry of Education and Science of Ukraine 0119U100777.

Pazukha I.M. – Ph.D (Physics and Mathematics), Associated Professor of the Electronics, General and Applied Physics Department;
Ovrutskiy M.S. – student;

Pylypenko O.V. – Ph.D (Physics and Mathematics), Senior Lecture of the Electronics, General and Applied Physics Department
Shuliarenko D.O. – Ph.D student;

Odnodvoretz L.V. – Dr.Sc (Physics and Mathematics), Professor of the Electronics, General and Applied Physics Department.

- [1] Ku Hoon Chung, Si Nyeon Kim, Sang Ho Lim, Thin Solid Films 650, 44 (2018) (<https://doi.org/10.1016/j.tsf.2018.01.062>).
- [2] A. Fert, F.N. Van Dau, Comptes Rendus Physique 20(7-8), 817 (2019) (<https://doi.org/10.1016/j.crhy.2019.05.020>).
- [3] I.M. Pazukha, Y.O. Shkurdoda, A.M. Chornous, L.V. Dekhtyaruk, International Journal of Modern Physics B 33, 1950113 (2019) (DOI: 10.1142/S0217979219501133).
- [4] L.V. Odnodvoretz, I.Yu. Protsenko, Yu.M. Shabelnyk, M.O. Shumakova, O.P. Tkach, Journal of Nano- and Electronic Physics 8(3), 03034 (2016) (DOI: 10.21272/jnep.8(3).03034).
- [5] S. Kumaraguru, R. Pavulraj, J. Vijayakumar, S. Mohan, S. Kumaraguru, R. Pavulraj, J. Vijayakumar, S. Mohan 693, 1143 (2017) (<https://doi.org/10.1016/j.jallcom.2016.10.027>).
- [6] Qian Liu, Shaolong Jiang, Jiao Teng, Journal of Magnetism and Magnetic Materials 454, 264 (2018) (<https://doi.org/10.1016/j.jmmm.2018.01.098>).
- [7] Umesh P. Borole, Sasikala Subramaniam, Ishan R. Kulkarni, P. Saravanan, Harish C. Barshilia, P. Chowdhury, Sensors and Actuators A: Physical 280, 125 (2018). (<https://doi.org/10.1016/j.sna.2018.07.022>).
- [8] Arnab Roy, P. Sampathkumar, P.S. Anil Kumar, Measurement 156, 107590 (2020) (<https://doi.org/10.1016/j.measurement.2020.107590>).
- [9] I.M. Pazukha, D.O. Shuliarenko, O.V. Pylypenko, L.V. Odnodvoretz, Journal of Magnetism and Magnetic Materials 485, 89 (2019) (<https://doi.org/10.1016/j.jmmm.2019.04.079>).
- [10] Yuan-Tsung Chen, Jiun-Yi Tseng, S.H. Lin, T.S. Sheu, Journal of Magnetism and Magnetic Materials 360, 87 (2014) (<http://dx.doi.org/10.1016/j.jmmm.2014.02.005>).
- [11] Guowen Ding, César Clavero, Daniel Schweigert, Minh Le, AIP Advances 5, 117234 (2015) (<http://dx.doi.org/10.1063/1.4936637>).
- [12] H.Y. Wan, X.M. Luo, X. Li, W. Liu, G.P. Zhang, Materials Science and Engineering A 676, 421 (2016) (<http://dx.doi.org/10.1016/j.msea.2016.09.010>).
- [13] Gesche Nahrwold, Jan M. Scholtyssek, Sandra Motl-Ziegler, Ole Albrecht, Ulrich Merkt, Guido Meier, Journal of Applied Physics 108, 013907 (2010) (<https://doi.org/10.1063/1.3431384>).
- [14] C.R. Tellier, A.J. Tosser, Size effects in thin films (Elsevier, 1982) (<https://doi.org/10.1016/B978-0-444-42106-7.50005-X>).

I.M. Пазуха, Д.О. Шуляренко, О.В. Пилипенко, М.С. Овруцький, Л.В. Оdnодворець

Концентраційні та розмірні ефекти в електрофізичних властивостях тонких плівок на основі пермалою та срібла

Сумський державний університет, Суми, Україна, iryana.pazukha@gmail.com

У роботі було проведено комплексне дослідження структурно-фазового стану та електрофізичні властивості тонкопліткових зразків на основі феромагнітного сплаву пермалою $\text{Ni}_{80}\text{Fe}_{20}$ та немагнітного металу Ag для широкого діапазону концентрації та у діапазоні товщин 20 - 100 нм. Для осадження тонкопліткових систем був використаний метод одночасної електронно-променевої конденсації за кімнатної температури. Хімічний склад і співвідношення концентрацій елементів контролювалися методом енергодисперсійного аналізу. Дослідження фазового складу зразків проводилося методами електронографії. Було показано, що фазовий стан пліткових систем залишається незмінним у процесі відпалювання до 500 К. Отримані концентраційні та розмірні залежності питомого опору та температурного коефіцієнту опору. Показано, що на концентраційних залежностях питомого опору та термічного коефіцієнту опору спостерігаються відповідні максимум і мінімум при концентрації немагнітної компоненти 50 - 60 ат.%. Характер розмірних залежностей питомого опору і термічного коефіцієнту опору пов'язаний з проявом розмірного ефекту у тонкопліткових матеріалах.

Ключові слова: тонка плівка, питомий опір, температурний коефіцієнт опору, розмірний ефект, концентраційний ефект.